JOURNAL OF SOLID STATE CHEMISTRY 81, 21–29 (1989)

Li-Inserted NbO_2F Studied by High-Resolution Electron Microscopy and X-Ray Powder Diffraction

LOTTA PERMÉR AND MONICA LUNDBERG

Department of Inorganic Chemistry, Arrhenius Laboratory, University of Stockholm, S-106 91 Stockholm, Sweden

Received December 22, 1988; in revised form February 27, 1989

Chemical insertion of Li in NbO_2F has been performed under various conditions. NbO_2F prepared from Nb-metal and a mixture of HF(aq) and HNO_3(aq) was used as starting material, since NbO_2F made from Nb_2O_5 and HF(aq) was shown to be $NbO_2F \cdot HF$. The products, with the formula Li_xNbO_2F ($0 < x \leq 1.8$), have been analyzed for Li content using atomic absorption spectrometry. According to the X-ray powder diffraction results, the Li-incorporated samples with $0.2 < x < 1.3$ contained two phases, namely, one of cubic and one of hexagonal symmetry, whereas specimens with $x > 1.3$ were single phase of a hexagonal structure type. Samples with $x = 0.0$, 0.3, 0.5, and 1.2 were studied by electron diffraction and high-resolution electron microscopy techniques. Crystals of specimen $x = 0.3$ were shown to consist predominantly of a cubic phase surrounded by a shell of hexagonal $LiNbO_3$ structure type, while the crystals of $Li_{1.2}NbO_2F$ seemed to be built up mainly of the hexagonal phase.

Introduction

Metal oxides with framework structures have in recent years become interesting as host compounds for Li-insertion, due to their potential use as electrode materials. Several articles describe Li-incorporation in ReO_3 (*1*, *2*) as well as other isostructural phases such as WO_3 (*2*), NbO_2F (*3*), and $TiOF_2$ (*3*). Their structures are built up of a three-dimensional network of corner-sharing MX_6 octahedra. The Li-inserted products obtained from these compounds seem to be structurally very similar, although small variations of the Li content have been observed. Studies of these systems using X-ray and neutron diffraction data show that one cubic phase of a distorted perovskite type and two hexagonal phases of $LiNbO_3$ type are formed. Li-insertion in metal oxides with shear structures, e.g., Nb_2O_5 (*4*, *5*) and Nb_3O_7F (*4*), have also been studied.

The present investigation has mainly been focused on topochemical incorporation of Li into NbO_2F. The products have been characterized by X-ray powder diffraction and high-resolution electron microscopy (HREM) methods.

Experimental

NbO_2F was synthesized by treating niobium metal powder (Pierce Inorganics B.V., 99.8%) with a mixture of HF(aq) (Merck, 48%, p.a.) and HNO_3(aq) (Merck, 65%, p.a.). The resulting clear liquid was left in room temperature for about 2 weeks for evaporation to dryness. The white crystals obtained were ground and heated in air

0022-4596/89 $3.00

at 550 K for 5 hr. Prior to use in the insertion reactions, the product was identified by X-ray powder diffraction and found to be a single-phase sample with good crystallinity. Its thermal stability was examined by differential scanning calorimetry (DSC, Perkin–Elmer DSC-2) and by thermogravimetric analysis (TG, Perkin–Elmer TGS-2).

Li was inserted chemically into the oxide fluoride by reaction with *n*-butyllithium dissolved in *n*-hexane (Merck-Schuchardt, 1.6 M, zur Synth.). All reactions were carried out in a drybox with N_2 atmosphere. Approximately 200 mg of NbO_2F was treated with 0.5–4 ml 1.6 *M* *n*-Bu–Li in *n*-hexane plus 10–20 ml pure *n*-hexane. The mixtures were stirred for 1–18 days at 295 K. The resulting dark blue or black crystals were washed three times in *n*-hexane and dried in vacuum for about an hour. The products were found to be unstable in air and were therefore all kept in the drybox. The starting material and Li-containing products were characterized by their X-ray powder diffraction photographs taken with a Guinier–Hägg camera using Cu$K\alpha_1$ radiation and Si as an internal standard (a = 5.430880(5) Å at 298 K (*6*)).

All products were analyzed with atomic absorption spectrometry (AAS) for Li content. Approximately 10 mg of the sample was dissolved in a small amount of HF(aq), and the solution was diluted with deionized water. Six water solutions of Li_2CO_3 (Baker Chemical Co.) with different concentrations were used as external standards.

Electron-microscope specimens were prepared by crushing a small amount of the sample under acetone in an agate mortar. Since the samples are sensitive to air and water the preparing times were minimized. Acetone was found not to react with the Li-containing crystals. These were examined at 125 kV using a Siemens ELMISKOP 102 with a double-tilt lift stage, at 200 kV using a JEM-200CX electron microscope equipped with a high-resolution top-entry goniometer stage, and at 400 kV using a JEM-4000EX electron microscope equipped with an ultra-high-resolution objective lens polepiece (C_s = 1.0 mm) and a top-entry goniometer stage. Simulated images were calculated with the multislice method, using a locally modified version of the SHRLI suite of programs (*7*).

Results

NbO_2F can be synthesized either by dissolving Nb_2O_5 in HF(aq) (*8*) or from Nb-metal as described above. The synthesis from Nb_2O_5 gave a sample with a structure of cubic symmetry with the cell parameter a = 3.9098(3) Å, yielding diffuse diffraction lines. According to (*9*) and references therein NbO_2F has a = 3.898 Å and starts to decompose at 825 K. However, the product here obtained started decomposing already at approximately 485 K. Thermogravimetric studies showed that the sample lost about 15 ± 2% in weight when heated to 573 K, at which temperature the cubic phase was still present according to the X-ray powder photograph. However, the a-axis shrank and the diffraction lines became more diffuse with the heat treatment of the sample.

When synthesized from Nb-metal the product had the same cubic structure type with a somewhat shorter a-axis (3.9015(1) Å). The powder pattern showed sharp diffraction lines, and major decomposition of the product did not occur until above 825 K. Thermogravimetric studies showed that this sample lost about 2% in weight when heated to 573 K, and the powder pattern did not change much in this process.

The 15 ± 2% weight loss suffered by the product obtained from Nb_2O_5 indicated a probable loss of one formula unit of HF or H_2O per NbO_2F (corresponding to full occupancy of the perovskite site). The theoretical weight loss in the two cases is 12 and 11%, respectively; thus a differentiating

test was needed. A Pt-crucible containing NbO_2F was covered with a piece of sodium glass and was exposed to the same heat treatment as in the TG experiment. The glass was etched when NbO_2F made from Nb_2O_5 was heated, indicating that HF was released, but was not at all affected by the product obtained from Nb-metal. The powder photographs confirmed that the residues were the same as those obtained in the thermogravimetric analyses. The behavior of the NbO_2F samples thus seemed to depend on whether it was made from Nb_2O_5 or from Nb-metal. The former sample apparently corresponds to the formula $NbO_2F \cdot HF$. Therefore all insertion reactions were made in NbO_2F synthesized from Nb-metal.

All insertion products with the formula Li_xNbO_2F ($0 < x < 2$) were examined by X-ray powder diffraction. It was observed that when Li was introduced into the cubic NbO_2F, the diffraction lines became diffuse. The powder patterns could be indexed, however, but the cell parameters could not be refined with high accuracy. The first appearance of a hexagonal phase could be observed for the sample with $x = 0.2$, although the major part of the specimen still consisted of the cubic phase. As x was increased the transformation became more pronounced, and for $x > 1.3$ the specimens were mainly single phase with a structure of hexagonal symmetry. The new phase could be recognized as being of the $LiNbO_3$ structure type described in (*10*). The Guinier film could be indexed, but since the diffraction lines were diffuse an accurate refinement of the unit cell parameters was not possible. For the cubic phase the unit cell volume was shown to decrease with increasing Li content from 59.4 Å^3 ($x = 0.0$) to 57.5 Å^3 ($x = 0.4$). This tendency is consistent with that observed in (*3*).

Four samples with different Li contents, viz., $x = 0.0$, 0.3, 0.5, and 1.2, were chosen for the EM studies. All Li-containing crystals were unstable in the electron beam, and it was shown that the instability increased with increasing Li content. Figure 1 shows a diffraction pattern with sharp reflections and a HREM image of a well-ordered crystal fragment of pure NbO_2F.

The electron diffraction (ED) patterns

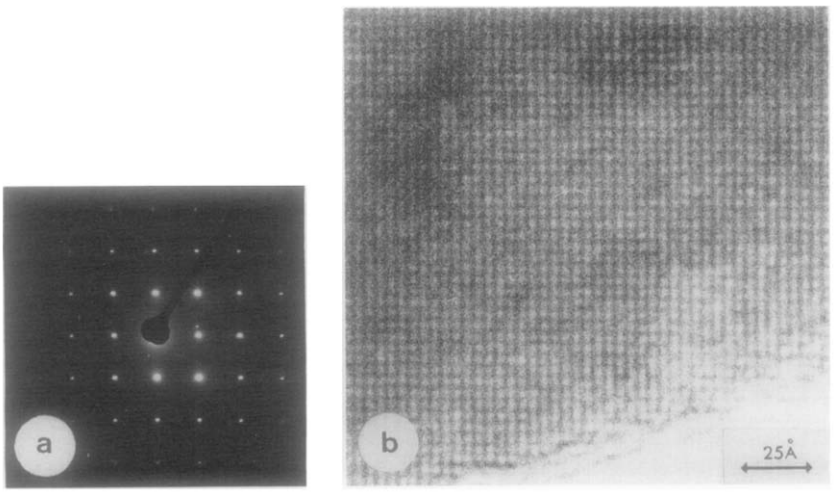

FIG. 1. (a) ED pattern of NbO_2F along [100] exhibiting sharp diffraction spots. (b) HREM image showing a well-ordered crystal. (Siemens ELMISKOP 102.)

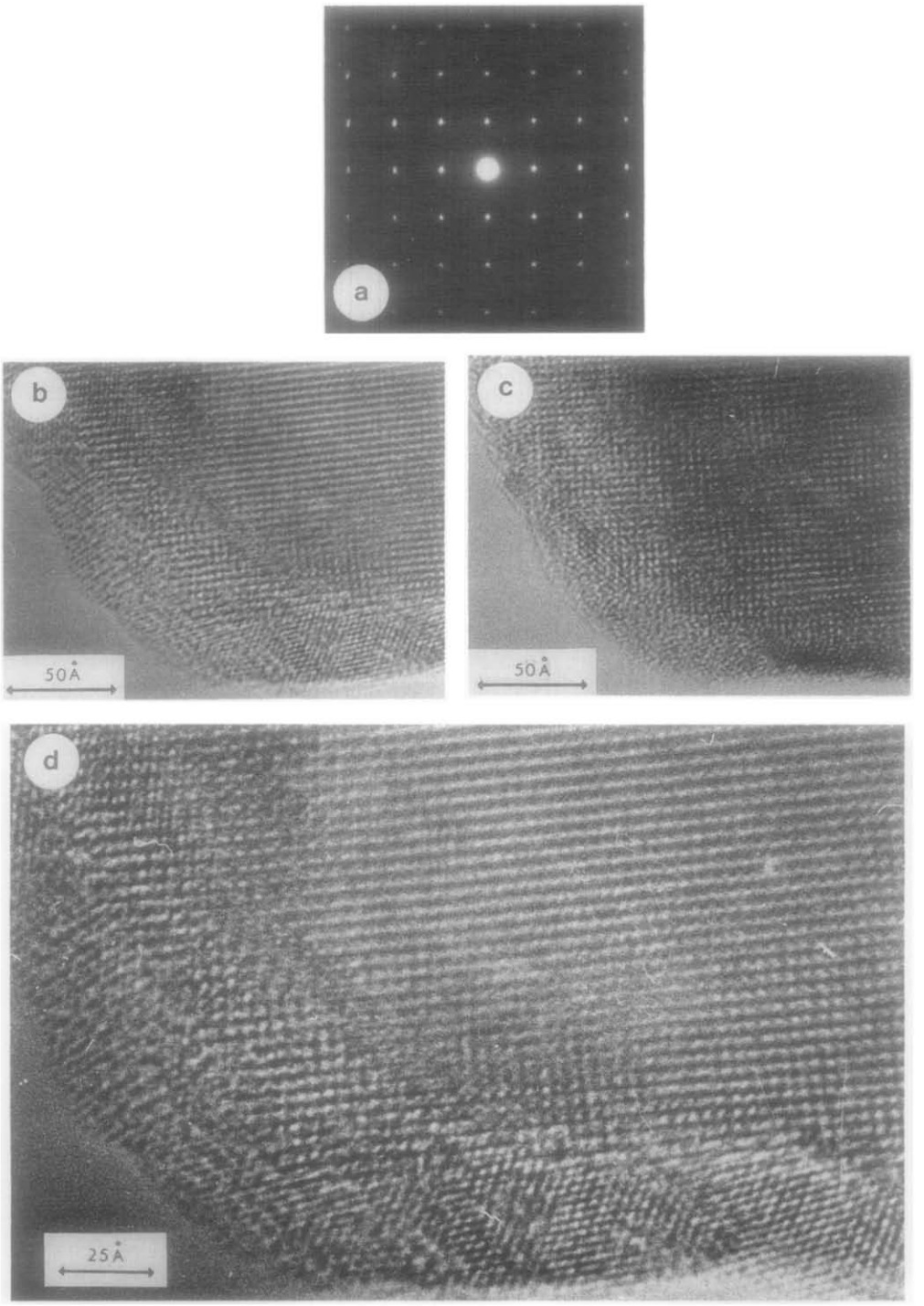

FIG. 2. (a) ED pattern of $Li_{0.3}NbO_2F$ indicating a crystal of cubic symmetry. (b) A low magnification of a fragment of cubic structure with a shell of hexagonally arranged metal atoms. (c) The same fragment after approximately 20 min, showing a diminished shell. (d) A larger magnification of (b). (JEM-4000EX.)

from the specimen with $x = 0.3$ are consistent with the crystals having cubic symmetry. The diffraction spots were relatively sharp as can be seen in Fig. 2a. HREM studies also showed that the crystals predominantly consisted of a well-ordered, apparently cubic structure. The outermost shell often looked amorphous, but in some cases a hexagonal structure could be observed. The hexagonal shell was destroyed; it shrank and finally disappeared during the exposure to the electron beam. In the end there was just a thin, amorphous shell growing into the cubic structure, and the crystals obtained looked like the ones on which no hexagonal shell could be detected.

The hexagonal shell of the $x = 0.3$ sample could best be studied with the 4000EX electron microscope. Figure 2b displays a lattice image of a fragment of $Li_{0.3}NbO_2F$, which mainly shows a simple square net corresponding to the metal atom arrangement. However, at the edge of the crystal there are areas within which atoms are hexagonally ordered. The width of the shell decreases with increased exposure time, as can be observed by comparing Figs. 2b and 2c. An enlargement of the edge of the crystal (cf. Fig. 2d) shows that the boundary between the cubic and hexagonal structures is disordered, as can be expected due to the mismatch between the two lattices. Despite this, a theoretical structure model comprising the $LiNbO_3$ structure type and the cubic framework of octahedra is given in Fig. 3. The repeat distance perpendicular to the projected plane of the computing model is taken as 39.3 Å, which corresponds to 10 layers of corner-sharing octahedra (3.93 Å each) in the cubic part and 17 layers of octahedra (2.31 Å each) in the hexagonal part, arranged in such a way that pairs of face-sharing octahedra are formed. The connection between the two structure types has been visualized by one slab of tilted and twisted octahedra, although the HREM images show that there are mostly more than one slab of displaced octahedra involved in the boundary and the rows of octahedra in the cubic phase are bent toward the hexagonal phase. It can also be observed that the angle between the two lattices changes along the edge of the crystal. In order to calculate the contrasts of the atoms in the coalescence of the cubic and hexagonal structures an ideal model of the lattices drawn parallel to each other has been constructed. Images were simulated by using atomic coordinates derived from the proposed structure model (Fig. 4). The projected unit cell axis (39.3 Å) was divided into slices 2.31 Å thick. By comparison of

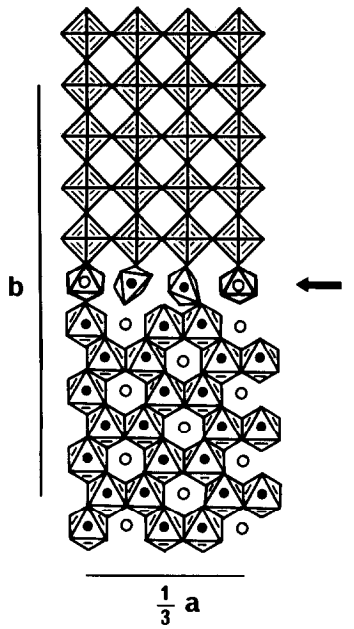

FIG. 3. One slice (2.31 Å) of the proposed structure model (a = 34.8 Å and b = 31.1 Å) comprising the connection between the cubic and the hexagonal structure types. The arrow marks a slab of tilted and twisted octahedra. Black dots = Li or Nb atoms. Fifty percent of the metal atoms (Li or Nb) in the six-membered rings of MX_6 octahedra belonging to the next layer are shown (open circles) in order to visualize the pattern of spots observed in Figs. 2b–2d. One-third of the a-axis of the model is depicted.

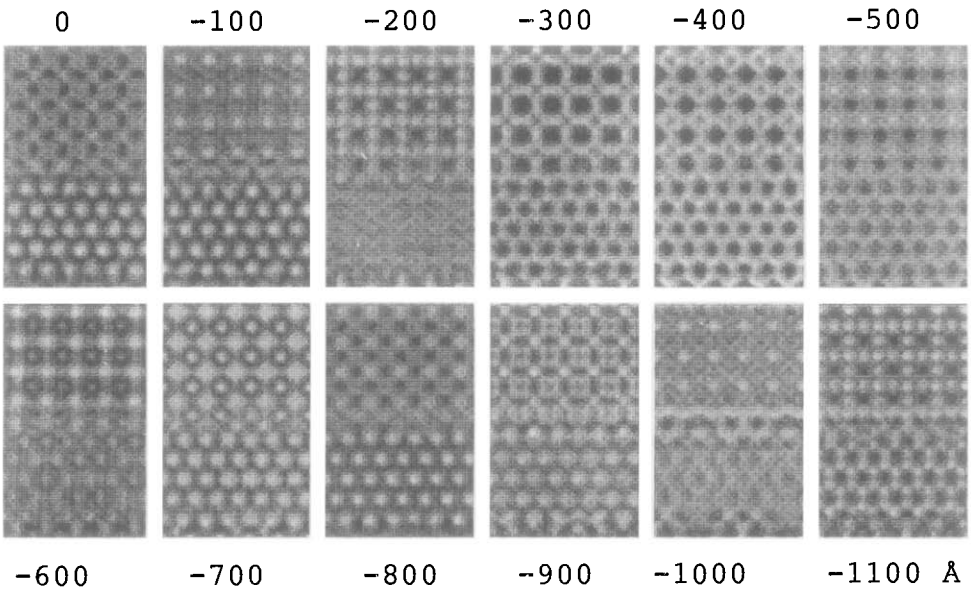

FIG. 4. Simulated images of the structure calculated as a periodic continuation of the model shown in Fig. 3. Accelerating voltage 400 kV, objective aperture corresponding to 1.0 $Å^{-1}$, C_s = 1.0 mm, beam convergens 0.50 mrad, and focus spread 30.0 Å. Crystal thickness 23 Å; slice thickness 2.31 Å.

the observed and calculated images quite a good match can be seen at a defocus value of −100 Å. The contrast is reversed in the simulated image of the hexagonal structure, while the atoms in the cubic structure appear dark and the four-sided tunnels white. At a defocus of −400 Å all atoms are black while at −1100 Å the contrast is reversed with respect to that at −100 Å. Thus, the choice of "best" defocus is ambiguous.

When studies of the specimen $x = 0.3$ were performed using the JEM-200CX, the crystals seemed to be sensitive to the beam. Fragments investigated along $[100]_c$ showed elongated diffraction spots in the ED patterns (Fig. 5a) while the reflections in the ED pattern along $[111]_c$ were relatively sharp (Fig. 6a). However, the HREM images in both directions revealed a high degree of disorder (Figs. 5b, 6b).

The sample with $x = 0.5$ appeared to be even more unstable in the beam. Here, too, the ED pattern showed that the crystals were built up of a cubic structure, but it was noticed that the diffraction spots became more diffuse with prolonged exposure to the electron beam. HREM images showed the same type of disordered cubic structure as for the sample with $x = 0.3$. However, the amorphous parts of the fragments were larger, and they steadily grew inward from the edge during the time in the beam. No hexagonal shell could be seen.

The last sample ($x = 1.2$) was very unstable and after approximately 30 sec the hexagonally shaped crystals turned into a totally amorphous state. Therefore, this specimen was difficult to study by this type of HREM technique. The ED pattern of a $Li_{1.2}NbO_2F$ crystal (Fig. 7) shows a characteristic hexagonal arrangement of the spots, which deviates from that calculated for the rhombohedral $LiNbO_3$ along the [111] direction. The hexagonal setting of the latter requires conditions for possible reflections $-h + k + l = 3n$, which is not fulfilled in the diffraction pattern of $Li_{1.2}NbO_2F$.

In order to determine to what extent the

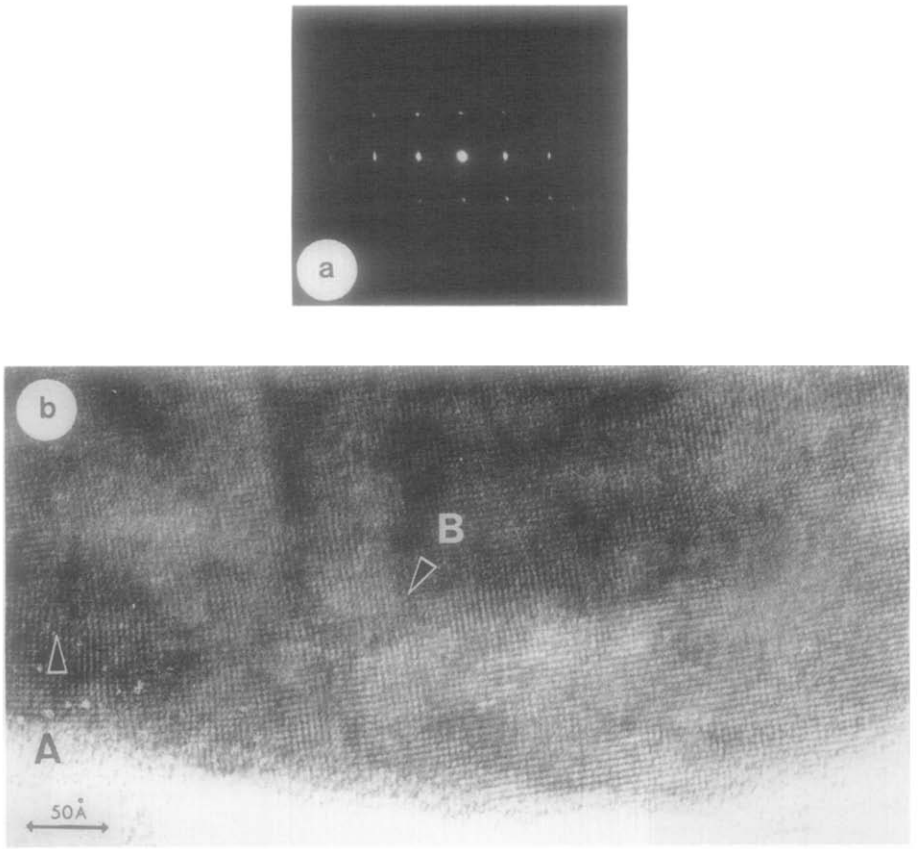

FIG. 5. (a) ED pattern of $Li_{0.3}NbO_2F$ along $[100]_c$ with elongated spots. (b) HREM image with a high degree of disorder. Rows of Nb atoms are disrupted (A) or curved (B). (JEM-200CX.)

Li content of the product was dependent of the reaction time and of the concentration of the Bu–Li solution, the insertion reactions were carried out under several different conditions. When 24 ml 0.27 *M* Bu–Li in *n*-hexane was allowed to react with the NbO_2F the Li content, *i.e.*, *x* in Li_xNbO_2F, increased from 0.8 after 1 day of reaction to 1.8 after 18 days. For solutions of lower concentration than 0.27 *M* the tendencies were the same, but after the same number of days the *x* values were always lower. However, a higher concentration, e.g., 14 ml 0.46 *M* Bu–Li in *n*-hexane, also gave lower *x* values (see Discussion).

Discussion

AAS was always used to analyze the insertion compounds for Li content. This method is simple, quite exact, and appears to be of good reproducibility. Other methods such as acid–base titration of excess Bu–Li or total delithiation with iodine in acetonitrile followed by an iodometric titration of excess iodine have also been tried ((*11*) and references therein). None of them was well reproducible, and the main problem with the delithiation method was to extract the total amount of Li. Further studies of the delithiation methods are in progress.

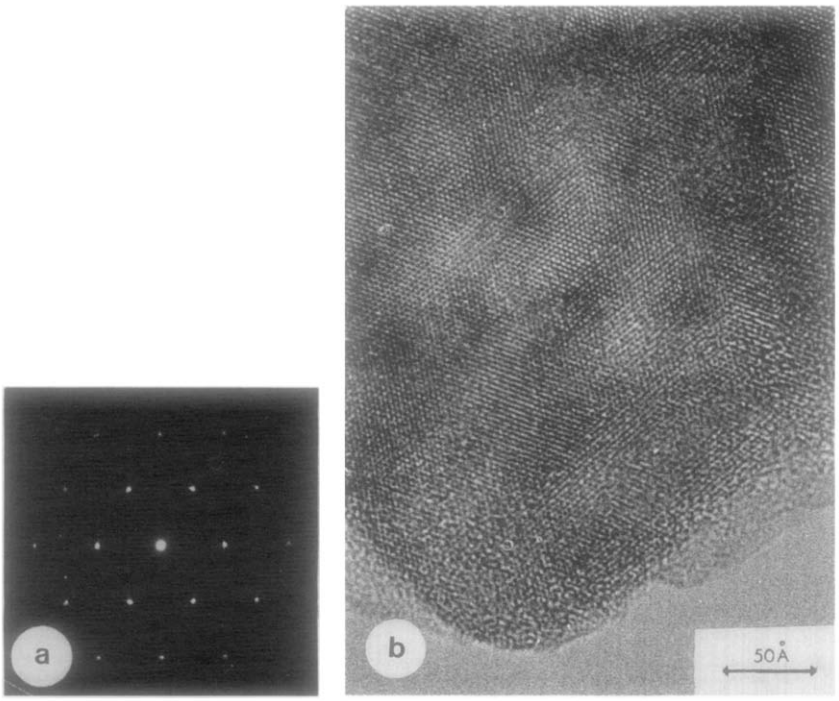

FIG. 6. (a) ED pattern of $Li_{0.3}NbO_2F$ along $[111]_c$. (b) Electron micrograph exhibiting a heavily disordered crystal flake projected along $[111]_c$. (JEM-200CX.)

The chemical insertion process implies a diffusion of foreign atoms into an existing structure. The Li atoms penetrating the structure can be thought of as distorting the lattice by forcing some of the metal atoms to move a little. This beginning of a structural transformation from cubic to hexagonal structure or amorphous state may give rise to the very diffuse lines in the X-ray powder diffraction patterns.

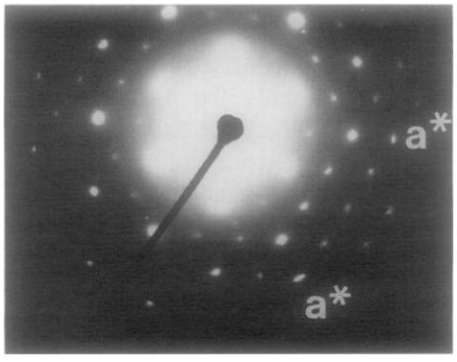

FIG. 7. ED pattern recorded from a crystal of the $Li_{1.2}NbO_2F$ sample showing diffuse spots in a hexagonal arrangement. (Siemens ELMISKOP 102.)

The Li content of the products seemed to depend on the particle size. When NbO_2F was carefully ground before use the x value increased for each particular combination of reaction time and Bu–Li concentration. It was further shown that the reproducibility of the Li content improved when the NbO_2F was ground to a smaller and more homogeneous particle size.

The maximum x value obtained was 1.8, which corresponds to 90% filling of the octahedral interstices available for Li in the approximately hexagonally close-packed anion structure. Theoretically it would be possible to insert 2 Li/M (M = transition

metal), which also has been reported for the Li_xReO_3 compound (*1*).

Since Li-incorporation is a surface reaction, it is natural to suggest that the outermost shell of the crystals should exhibit higher Li content than the central part, which is in agreement with the HREM studies (cf. Fig. 2). The formation of a shell of hexagonal structure around the relatively undistorted cubic one might explain the fact that solutions of high Bu–Li concentration gave lower x values. The higher the concentration of the solution, the quicker this shell was formed and the slower the diffusion of more Li atoms into the particles.

Only a small fraction of the fragments examined showed this kind of edge structure and it seems likely that these represent the original surface of the crushed crystals.

The hexagonal structure seen in the HREM images could be any niobium compound with hexagonal symmetry. However, the X-ray powder diffraction shows that the new structure obtained is of the $LiNbO_3$ type.

A proposed structure model of the connection between the cubic NbO_2F projected along $[100]_c$ and the hexagonal "$LiNbO_3$" along $[001]_h$ is given in Fig. 3. According to the observed HREM images, the width of the disordered area between the two structure types varies (Fig. 2). However, the aim of the model is to demonstrate a possible way of connecting the two different polyhedral frameworks through a few distorted and tilted octahedra. The proposed model for the transformation from a cubic to a close-packed hexagonal structure of Li_xReO_3 given by Cava *et al.* (*1*) corresponds to a rotation of approximately 60° about the cubic ⟨111⟩ direction, which presumes that $\langle 111\rangle_c$ is parallel to the $\langle 001\rangle_h$ direction. However, from the HREM images of Li_xNbO_2F the transformation mechanism seems to be of a different kind, as the $\langle 100\rangle_c$ and $\langle 001\rangle_h$ directions are parallel, although both models involve twisting of octahedra.

Results concerning the thermal stability of the insertion compounds will soon be published elsewhere.

Acknowledgments

Valuable discussions with Professor M. Nygren are gratefully acknowledged. We thank Professor L. Kihlborg for profitable comments on the manuscript. We also thank Drs. J.-O. Bovin and R. Wallenberg for their skillful help in taking the photographs with the JEM-4000EX electron microscope. This work has been supported by the Swedish Natural Science Research Council.

References

1. R. J. Cava, A. Santoro, D. W. Murphy, S. Zahurak, and R. S. Roth, *J. Solid State Chem.* **42,** 251 (1982).
2. R. J. Cava, A. Santoro, D. W. Murphy, S. Zahurak, and R. S. Roth, *J. Solid State Chem.* **50,** 121 (1983).
3. D. W. Murphy, M. Greenblatt, R. J. Cava, and S. M. Zahurak, *Solid State Ionics* **5,** 327 (1981).
4. R. J. Cava, D. W. Murphy, and S. M. Zahurak, *J. Electrochem. Soc.* **130,** 2345 (1983).
5. W. Sahle and M. Nygren, *Ultramicroscopy* **24,** 65 (1988).
6. C. R. Hubbard, H. E. Swanson, and F. A. Mauer, *J. Appl. Crystallogr.* **8,** 45 (1975).
7. M. O'Keefe, P. R. Buseck, and S. Iijima, *Nature (London)* **274,** 322 (1978).
8. L. K. Frevel and H. W. Rinn, *Acta Crystallogr.* **9,** 626 (1956).
9. S. Andersson and A. Åström, *Acta Chem. Scand.* **19,** 2136 (1965).
10. Y. Shiozaki and T. Mitsui, *J. Phys. Chem. Solids* **24,** 1057 (1963).
11. D. W. Murphy and P. A. Christian, *Science* **205,** 651 (1979).